

Collective light forces on atoms in resonators

Adam T Black, James K Thompson and Vladan Vuletić

Department of Physics, MIT-Harvard Center for Ultracold Atoms, and Research Laboratory of Electronics, Massachusetts Institute of Technology, Cambridge, MA 02139, USA

E-mail: vuletic@mit.edu

Received 29 December 2004

Published 25 April 2005

Online at stacks.iop.org/JPhysB/38/S605

Abstract

We study resonator-induced light forces arising from cooperative atom–light interaction. For such collective processes, the force on the sample can be orders of magnitude larger than the sum of conventional light forces on individual atoms. Since resonator-induced light forces can be dissipative even when the incident light is far detuned from atomic transitions, they may be applicable to target particles with a complex level structure.

(Some figures in this article are in colour only in the electronic version)

1. Introduction

Atomic physics, being perhaps the most ‘quantum’ field of all experimental physics, is to a large extent built upon foundations laid out by Albert Einstein almost a century ago. The Holy Grail of atomic physics, Bose–Einstein condensation [1, 2] in a dilute atomic gas, achieved in 1995 [3–6], owes perhaps as much of its public appeal to its intriguing properties as to the Einstein name. While only ten years ago atomic physics had largely been concerned with single-particle quantum processes, Bose–Einstein condensation has introduced intriguing many-body properties [7] that are, in part, redefining the field. Furthermore, many of the processes and tools of modern atomic physics are based on concepts introduced by Einstein almost 100 years ago. Einstein’s A and B coefficients [8], or the distinction between spontaneous and stimulated quantum processes, can be invoked to explain not only the macroscopic population of the ground state in a Bose–Einstein condensate, but also the working principle of the optical laser used to cool the atoms. In laser cooling [9–11], the Brownian motion and diffusion [12] in momentum space arise from the quantized momentum of the photon [8]. The corresponding heating of the atoms that accompanies the dissipative force in optical molasses [13] determines the final atomic temperature.

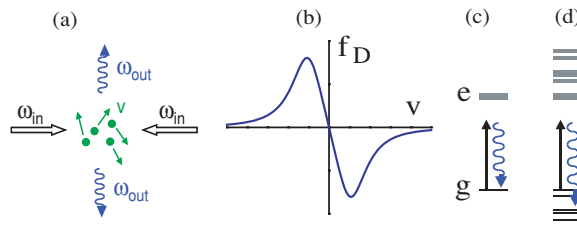


Figure 1. Conventional Doppler cooling. (a) A thermal atomic sample is irradiated with monochromatic laser light of frequency ω_{in} and scatters photons of various frequencies ω_{out} into free space. If the average emission frequency $\langle\omega_{\text{out}}\rangle$ exceeds that of the incident light, the sample is cooled. (b) Doppler cooling force f_D as a function of atomic velocity. (c) For Doppler cooling two-level atoms with ground state g and excited state e are irradiated by light red detuned by an amount comparable to the Doppler effect relative to the atomic transition. (d) Doppler cooling cannot be applied to atoms with many internal states because the condition on the detuning cannot be maintained simultaneously for different levels.

2. Laser cooling in optical resonators

2.1. Cooling force and resonator emission

Already in the early days of laser cooling, Mossberg, Lewenstein and Gauthier [14] pointed out that the light forces on atoms are modified inside an electromagnetic vacuum with a frequency-dependent mode density, i.e. inside an optical resonator. This question of general interest has been analysed further in considerable detail by Helmut Ritsch and co-workers (see, for example, references [15–18], and references therein). Much of the recent experimental work on resonator-induced light forces [19–24] has been motivated by the search for a generalized laser cooling method that could be extended to new atomic or molecular species [15, 25]. Obviously, the target atom needs to interact with the applied light in order to be cooled, and the dissipative force will scale with the strength of the atom–light interaction. However, it would be of great advantage to find methods that, while depending on the polarizability of the particle, do not require the target to possess a closed optical transition between two levels.

To identify general requirements for laser cooling, consider an atomic sample interacting with monochromatic incident light of angular frequency ω_{in} (figure 1(a)). We assume that non-radiative decay processes are negligible, i.e. for each incident photon a photon of some, in general different, frequency ω_{out} leaves the sample. Then energy conservation implies that the sample will be cooled if the average frequency of the emerging light $\langle\omega_{\text{out}}\rangle$ exceeds the frequency ω_{in} of the incident light. While in general cooling, i.e. a reduction of the phase space volume occupied by the sample, requires a reduction in entropy, and not merely in energy, for a stationary thermal sample a reduction in energy implies a reduction in entropy, and the above energy criterion is sufficient to ensure cooling.

In conventional laser cooling [11], the condition $\langle\omega_{\text{out}}\rangle > \omega_{\text{in}}$ is achieved by means of the detuning of the incident light relative to an atomic transition. For instance, in Doppler cooling [9] the incident light is tuned below the atomic resonance by an amount comparable to the Doppler effect of the moving particle (figure 1(c)). Then the scattering process where the moving atom scatters an incident photon from a laser beam directed against its motion into free space has a smaller detuning from the intermediate excited atomic state, and therefore a larger rate, than a process where the atom scatters a photon from a beam directed along its direction of motion. The resulting average force f_D , directed against the atom's direction

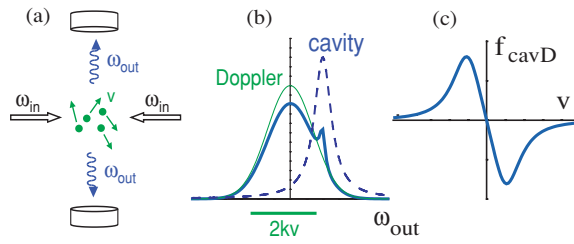


Figure 2. Cavity Doppler cooling. (a) The sample is placed inside an optical resonator blue detuned relative to the incident light. (b) The spectrum of the light emitted into free space is approximately symmetrically Doppler broadened (thin line). The spectrum including the emission into the resonator is asymmetric because the resonator enhances the emission in proportion to its lineshape (thick line). (c) Cavity Doppler force $f_{\text{cav}D}$ with typical velocity dependence.

of motion, is dissipative, and cools the atom (figure 1(b)). However, Doppler cooling is not applicable to particles with multiple ground states because the light–atom detuning will differ for different ground states (figure 1(d)).

Nevertheless, inside an optical resonator a very similar dissipative Doppler force can be attained even for multilevel atoms (figure 2) [25, 26]. We assume that the incident light is far detuned from atomic resonances. Then the photon scattering rate into free space is independent of the atom’s velocity, and the light scattered by the thermal gas has an approximately symmetrically Doppler-broadened spectrum (figure 2(b), thin line). In contrast, the resonator with its frequency-dependent electromagnetic mode density (dashed line) enhances the scattering of light near its resonance frequency (the Purcell effect [27]), rendering the emission spectrum asymmetric (figure 2(b), thick line). Then if the optical resonator is tuned to the blue of the incident light by an amount comparable to the Doppler effect of the thermal gas, the average emission frequency into the resonator will exceed that of the incident light. This results in a cooling force $f_{\text{cav}D}$ with a velocity dependence typical of the Doppler force (cavity Doppler cooling) (figure 2(c)) [25, 26].

The cavity Doppler force exists independent of the atom’s level structure as long as the atom–light interaction can be described by classical coherent scattering. If the light is tuned close to an atomic transition, then the variation of the dissipative force with light–atom and light–cavity detuning is much more complex, as has been analysed in [14–16, 18], and observed for a single atom strongly coupled with a resonator [24]. We also note that the asymmetry in the emission spectrum necessary for cooling can be induced by mechanisms other than the resonator–light detuning. Rather, any process that leads to an asymmetric Doppler emission spectrum with stronger blue than red emission will cool the scatterer, even when the resonator electromagnetic mode density does not vary strongly with frequency.

The force on the atom arises from the photon momentum transfer [8] in the scattering process, and consequently the cooling force will be proportional to the photon scattering rate into the resonator. A useful parameter to quantify the latter for a single atom is the cavity-to-free-space scattering ratio η , defined as the fraction of photons emitted into one direction of the resonant cavity, compared to the total scattering into free space in the absence of the resonator. For an atom on the cavity axis illuminated by light incident and polarized perpendicular to the cavity axis, the cavity-to-free-space scattering ratio into a TEM_{00} mode is given by $\eta = 6F/(\pi k^2 w^2)$, where F is the finesse of the cavity, k is the wavenumber of the light, and w is the mode waist size [26]. This expression is easily interpreted as the product of the far-field solid angle $\Delta\Omega = 3/(k^2 w^2)$ subtended by the cavity mode, and the power enhancement F/π of the resonant cavity. The cavity-to-free-space scattering ratio η is the

same quantity as the single-atom cooperativity $g^2/(\kappa\Gamma)$ in cavity quantum electrodynamics (cavity QED), where g is the single-photon Rabi frequency of the resonator, κ is the resonator linewidth, and Γ is the atomic linewidth. However, the expression for the cavity-to-free-space scattering ratio displays more clearly its geometric origin, and its significance for scattering forces. For instance, η takes on the same value for resonators of different length with the same mirror reflectivity and mode waist size. Expressed in terms of η , the maximum single-atom scattering force can be of order $\hbar k\eta\Gamma_{\text{sc}}$, where $\hbar k$ is the photon momentum, and Γ_{sc} is the atom's photon scattering rate into free space. Since the scattering force can already be substantial for $\eta < 1$, it follows that the observation of resonator-induced light forces does not require the very short cavities used typically in cavity QED to attain the strong-coupling limit $g \gg \kappa, \Gamma$ (see, for instance, [24, 28, 29]).

2.2. Collective light forces

Resonator-induced forces become significantly more complex and intriguing if the emission by a probe atom is influenced by the presence, position and velocity of other atoms inside the resonator. For instance, in lasers the photon emission rate per atom into the resonator is no longer governed by Einstein's A coefficient, but by the much larger stimulated emission term Bn , where n is the number of photons inside the resonator [8]. Similarly, in Dicke superradiance [30] from an N -atom sample [31] or a Bose–Einstein condensate [32, 33] the photon emission rate per atom can be enhanced by a factor of order N due to constructive interference of the fields emitted by different atoms. Since each emission event is associated with the transfer of momentum onto the atom, collectively enhanced photon emission implies the possibility of collectively enhanced light forces. Such forces could exceed conventional single-atom forces by a large factor, given by the number of photons or atoms participating in the emission. Collectively enhanced light forces have not been observed in conventional laser cooling, where the dissipative mechanism is a single-atom process, and the presence of other atoms only deteriorates the cooling performance [11].

Recently several experiments have investigated mechanical effects on atomic samples in the regime of strong collective light–atom coupling. For scattering processes, this regime can be characterized by the condition $N\eta > 1$. The condition $N\eta > 1$, or the *collective cooperativity* $Ng^2/(\kappa\Gamma)$ exceeding unity in the language of cavity QED, corresponds to the threshold for overdamped superradiance [31]. In this regime, the cooperative emission by the N atoms into the resonator mode at rate of order $N^2\eta\Gamma_{\text{sc}}$ [30] can exceed the emission into all of free space, that leads to a decoherence of the collective state at a rate $N\Gamma_{\text{sc}}$. For a free-space scattering rate per atom Γ_{sc} less than the resonator linewidth κ , the condition $N\eta > 1$ is less stringent than the condition $N\eta\Gamma_{\text{sc}} > \kappa$ where ringing superradiance, i.e. coherent oscillatory exchange of the excitation between the sample and the cavity is observed [34].

Recent experiments on optical bistability induced by the mechanical motion of atoms [20] operate in the regime $N\eta\Gamma_{\text{sc}} > \Delta_0$, where $\hbar\Delta_0$ is the optical potential experienced by the atoms. In this regime the maximum dispersive shift δ_N of the resonator mode by the sample, of order $\delta_N \sim N\eta\Gamma_{\text{sc}}\kappa/\Delta_0$, exceeds the cavity linewidth κ , and cooperative motion of the atoms inside the cavity can turn the resonator transmission on and off (see section 3.4).

3. Collective forces for two-level atoms

All recent experiments studying forces on atomic samples in resonators [19–22] have been performed with atoms with non-zero nuclear spin, i.e. with atoms that possess multiple

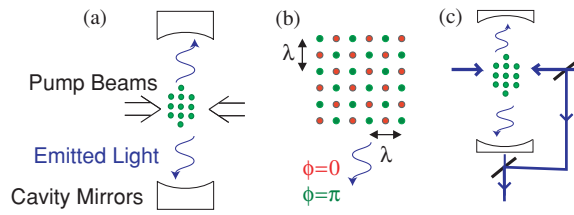


Figure 3. Collective spatial self-organization of two-level atoms and emitted light. (a) The atoms inside a vertical optical resonator are illuminated with a horizontal, horizontally polarized standing wave. Above a certain threshold pump intensity, strong emission into the resonator is observed. (b) The atoms can self-organize into one of two equivalent, but spatially offset gratings. The time phase of the Bragg scattered light differs by π between the two gratings. (c) Interferometric setup to observe the time phase of the Bragg scattered light and the atomic density grating. A portion of the pump beam is overlapped with the light exiting the resonator to measure the time phase of the Bragg scattered light.

hyperfine and magnetic ground states. Optical pumping associated with the different Clebsch–Gordan coefficients leads to different sublevel populations. The ensemble can then provide optical gain associated with the inversion between different atomic ground states (see section 4). The simplest situation, however, arises when the detuning of the laser from the relevant atomic transitions far exceeds the atomic (excited-state) hyperfine structure. In this case the different magnetic sublevels are equally populated, and the atoms can be approximated as two-level atoms, or, at not too high intensity, as classical polarizable particles.

3.1. Spatial self-organization, Bragg scattering and collective centre-of-mass cooling

Consider a sample of polarizable particles inside a vertical cavity that is illuminated from the side with two counterpropagating laser beams (pump beams) linearly polarized in the horizontal plane (figure 3(a)). We observe that above a certain threshold intensity of the pump beams, the light scattering by the sample into the cavity increases dramatically, with up to 10^4 times more light scattered into the cavity than by a sample of independent emitters [22, 35]. This strong cavity emission is all the more surprising, as the large detuning precludes the existence of any hidden optical gain in the atoms' internal degrees of freedom, e.g., in the form of Raman gain between differently populated magnetic sublevels (see section 4). Therefore the collective emission by the atoms in the sample must be due to spatial, rather than internal, degrees of freedom.

In subsequent numerical simulations Domokos and Ritsch [17] found that for sufficiently strong pump beams even small samples of atoms self-organize into stable periodic patterns anchored at the antinodes of the resonator standing wave. These atomic density gratings then Bragg scatter light into the resonator, with a rate that increases as the square of the atom number N . The self-organization of atoms and light constitutes a run-away process: the interference of the scattered light with the incident field creates an optical lattice that tends to localize the atoms via the ac Stark shift. The bunching of the atoms in the periodic potential increases the scattering into the cavity, which in turn deepens the optical lattice. An interesting feature of the self-organization process, necessary for constructive interference in the Bragg scattering, is that the atoms must self-organize into a grating of period λ , instead of the $\lambda/2$ period of the standing wave. As there are two such equivalent, but spatially offset gratings (figure 3(b)), the atoms spontaneously break the symmetry and choose one of the gratings to self-assemble into [17].

Since the two possible lattices are shifted along the cavity axis by a distance $\lambda/2$, they can be distinguished via the time phase of the Bragg scattered light. To observe this phase,

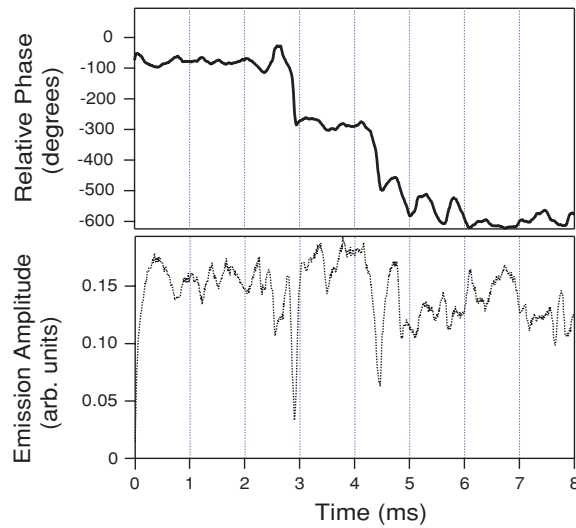


Figure 4. (a) Time phase of the Bragg scattered light displaying the transition between two spatially shifted Bragg gratings. (b) The power emitted into the cavity decreases during the time that the atoms are reorganizing from one grating into the other.

we use a heterodyne technique where we superimpose the light exiting the cavity with a frequency-shifted portion of the pump light, thereby forming a Mach–Zehnder interferometer with the atomic Bragg grating acting as one mirror (figure 3(c)). We observe that the phase of the cavity light exhibits portions of approximately constant phase, interrupted by sudden jumps of magnitude π , that correspond to reorganization of the atomic sample into a spatially shifted lattice (figure 4(a)). Simultaneously with the phase jumps, the Bragg scattered power decreases while the atoms are self-organizing into the new lattice (figure 4(b)) [22].

The above observations of a stationary atomic density grating were made by illuminating an atomic cloud at rest. If instead a cloud falling at velocity v along the resonator axis is prepared, we observe the collective emission of two frequency components separated by $2kv$. The two components correspond to the downward and upward emitted light, shifted by $\pm kv$ relative to the monochromatic pump light [22]. As figure 5(a) shows, the sideband separation, observed as a beatnote on a photodiode, decreases during the collective emission, indicating a reduction of the cloud's velocity. The deceleration can also be observed in time-of-flight measurements, where up to a third of the original falling cloud is stopped (figure 5(b)). The collective-emission-induced force is a friction force acting on the centre-of-mass motion of the atomic cloud, since it brings the cloud to rest, independent of the sample's initial velocity. The observed centre-of-mass decelerations, with values up to 3000 m s^{-2} , are comparable to the maximum conventional Doppler deceleration. However, the collective decelerations were achieved at quite small atomic saturation $p \approx 10^{-2}$, and consequently quite small single-atom Rayleigh scattering rate $\Gamma_{\text{sc}} = p\Gamma/2 \approx 10^5 \text{ s}^{-1}$. Therefore we expect to be able to significantly further increase the collective friction force using more powerful pump beams (see section 3.2). Furthermore, for cooling multilevel particles the collective forces have the great advantage that the collective Rayleigh rate, i.e. the scattering rate where the atom returns to its initial internal state, is significantly increased compared to spontaneous Raman transitions that take an individual atom to a different internal level. This means that for a given saturation of the atomic transition, and therefore excited-state population, one can obtain significant momentum transfer onto the atom even on an open transition [36].

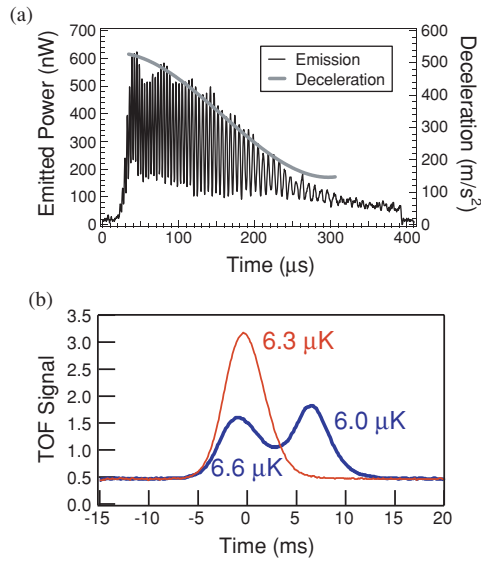


Figure 5. Centre-of-mass deceleration of a falling atomic cloud. (a) The power emitted by a falling atomic cloud (thin line). The change in the frequency of the beatnote at $2kv$ is used to calculate the deceleration (thick line). (b) Time-of-flight measurement showing the falling cloud without exposure to the pump beam (single peak), and the decelerated and undecelerated components when the pump beam is applied. The initial cloud temperature and the final temperatures of the delayed cloud and the undelayed remnant are indicated.

Further refining the model from [17], Zippilli *et al* arrive at some very interesting additional predictions [37]. For instance, as the atom number is increased, the cavity emission is predicted to first increase and then saturate. In the saturation region, the excitation of the atom by the strong intracavity light interferes destructively with the excitation by the pump light, which should lead to a reduction of the excited-state population, and of the emission into free space. Therefore the cavity-to-free-space scattering ratio is predicted to continue to increase with atom number in spite of the saturation of the cavity emission. This may be important for the cooling on an open transition, since the reduced population of the excited state also corresponds to a lower optical pumping rate into other ground states of the target particles, where the scattering rate, and the light force, may be smaller.

3.2. Prospects for the stopping of a molecular beam

One may ask if it is possible and realistic to use collective light forces to stop a molecular beam. The largest deceleration we have attained in the present setup is $a = 3 \times 10^3 \text{ m s}^{-2}$, observed at a saturation parameter of $p = 10^{-2}$, and a cavity photon emission rate per atom of $\Gamma_{\text{cav}} \approx 5 \times 10^6$ [36]. These observations were made for slow samples, where the centre-of-mass velocities of typically 0.2 m s^{-1} corresponds to a Doppler effect $2kv/(2\pi) = 0.5 \text{ MHz}$ that is smaller than the cavity linewidth $\kappa/(2\pi) = 1 \text{ MHz}$. Then both the red and the blue Doppler sideband are supported by the cavity. One may expect that in the opposite case of a fast-moving sample, $2kv \gg \kappa$, where the cavity is tuned such that only the blue Doppler sideband is resonant, the red sideband would not be collectively enhanced. In this case all photons emitted into the resonator would contribute to the cooling of the centre-of-mass motion, and the deceleration for the same parameters should be approximately six times larger than observed.

We are setting up an experiment where we are using a moving-molasses technique [11], i.e., a light trap with frequency-shifted cooling beams, to prepare a cold-atom beam with cloud velocities exceeding 1 m s^{-1} . This would enable us to probe the collective light force in the regime where only one Doppler sideband is resonant with the cavity. If in this case the damping force is close to its maximum possible value, then the light-induced stopping of a fast molecular beam seems well within reach. In that case the maximum collective light force acting on the sample's centre-of-mass motion can be estimated as follows: the maximum coherent scattering rate is $\Gamma_{\text{sc}} = \Gamma/4$, where Γ is the atomic linewidth, and the corresponding maximum atom deceleration is $a_{\text{max}} = N\eta v_{\text{rec}}\Gamma_{\text{sc}} = 3 \times 10^7 \text{ m s}^{-2}$ for a caesium sample with a typical observed value $N\eta = 100$, where $v_{\text{rec}} = 3.5 \text{ mm s}^{-1}$ is the recoil velocity for caesium. The corresponding stopping distance for a beam with initial velocity $v_0 = 180 \text{ m s}^{-1}$, corresponding to the thermal velocity at 500 K, is $s = v_0^2/(2a_{\text{max}}) = 5 \text{ mm}$, sufficiently short to fit inside an optical resonator. Larger atom number in the beam leads to faster slowing, and for $N\eta = 1000$ the stopping distance reduces to $500 \mu\text{m}$.

Given that the threshold for self-organization and collective emission depends on the temperature in the moving frame [36], a favourable system is a supersonic beam, since the sample's temperature can be below 1 K in the moving frame. The supersonic beam has the additional advantage that the molecules would be prepared in a single rotational–vibrational level, and the polarizability near a single strong transition can be large. Both features make it easier to reach threshold for collective emission. Note also that since the Bragg scattering (collective Rayleigh scattering) back to the initial state exceeds the free-space scattering by a large factor, it is possible to exert a large impulse onto the sample even on an open transition.

3.3. Collective atomic recoil laser and accelerating samples

In experiments with a sample of ultracold atoms inside a unidirectionally pumped high-finesse ring resonator, Kruse *et al* have observed the buildup of a frequency-shifted reverse field [21]. This process is accompanied by a strong acceleration of the sample induced by a collective-emission force. This force has been attributed to, and analysed in terms of [38], the collective atomic recoil laser (CARL) [39, 40]. Above a certain threshold pump power of the running wave inside the ring resonator, the atoms start to collectively backscatter light by bunching into a density grating. The momentum imparted to the backscattered light field produces a strong collective forward force on the atoms that accelerates the atomic sample [21], unless it is counteracted by an external friction force that results in a steady-state velocity and CARL emission frequency [38].

It is interesting to analyse the steady state of CARL in two complementary pictures. In the position basis, the generated backward propagating light wave is due to the Bragg scattering of the incident coherent beam off the moving atomic density grating. From this viewpoint, the generated light field is coherent because it is simply a coherent wave reflected off a moving Bragg mirror that is accelerated due to light pressure. In the momentum basis, the generated light can be viewed as being due to the Raman lasing between momentum states where atoms make a Raman transition from a state with momentum p to a less populated state with momentum $p + 2\hbar k$. Thus, as already discussed by Courtois *et al* in the context of recoil-induced resonances [42], the process can be alternatively viewed as Bragg scattering or Raman gain. The main novel and interesting feature of the recent work is that in [42] both a pump and a probe laser were applied, while in the CARL experiments [21, 38] the probe field and the atomic bunching are self-generated.

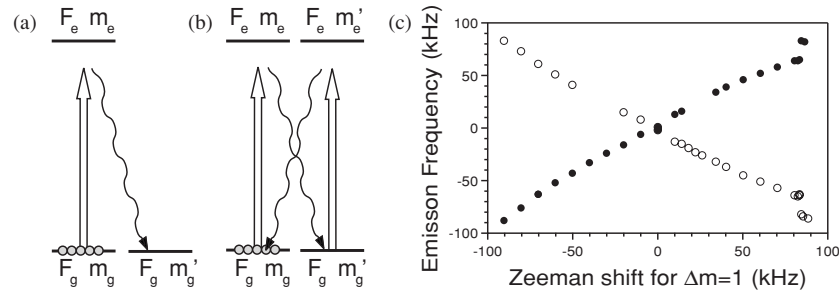


Figure 6. The multiphoton processes involved in (a) Raman gain between two magnetic sublevels and (b) four-wave mixing gain using different magnetic sublevels as the intermediate states. The multilevel nature of the collective emission is demonstrated by the magnetic-field dependence of the frequencies (c) of circularly polarized σ^+ (closed circles) and σ^- (open circles) emitted light.

3.4. Optical bistability due to collective atomic motion

In very interesting experiments combining mechanical effects on atoms with optical bistability in a nonlinear system, Nagorny *et al* have observed collective nonlinear dynamics in a very simple setup [20]. Cold atoms are prepared inside a ring resonator whose running modes are pumped by two independent beams derived from the same laser. The cavity is locked to one of the beams with a very fast servo loop, while the transmission of the second beam through the resonator is measured. Surprisingly, if the intensities of the two input beams differ by an amount as small as 1%, the second, unlocked beam is completely reflected from the cavity. When the atoms slowly leave the cavity, reducing the collective cooperativity $N\eta$, the transmission of the unlocked mode suddenly jumps back to its unperturbed value.

The behaviour can be understood in terms of the normal modes of the resonator [41], where the periodic atomic sample confined in the lattice couples the two running modes via backward Bragg scattering. The two new normal modes correspond to optical lattices that are spatially shifted with respect to one another. These normal modes couple with different strength to the atomic sample, and are consequently non-degenerate in frequency. This explains why one beam can remain coupled into the resonator while another beam of the same frequency is reflected. The system is inherently non-linear since the localization of the atoms depends on the lattice depth, that in turn depends on the Bragg scattering by the localized atomic sample. For a certain range of parameters, the system exhibits optical bistability associated with the collective motion of the atomic sample [20, 41].

4. Collective forces for multilevel atoms

The most complex situation arises for light–atom detunings comparable to or smaller than the atomic hyperfine structure, where the multilevel structure of the atoms must be taken into account. In this case spontaneous Raman scattering into free space, that occurs at different rates for the different magnetic sublevels, leads to population differences between these levels. The population differences can then give rise to stimulated Raman gain when the atom emits light into the cavity on a transition $|F_g, m_g\rangle \rightarrow |F_e, m_e\rangle \rightarrow |F_g, m_g'\rangle$ (figure 6(a)). If the corresponding optical round-trip gain is sufficiently large to overcome cavity losses, the atom–cavity system can act as a Raman laser, particularly if the light polarizations are chosen such that the Rayleigh emission and the Rayleigh superradiance (section 3.1) into the cavity cannot occur. (Similar Raman gain and Raman superradiance have also been

observed without a resonator in an elongated Bose–Einstein condensate [33].) In addition, the population difference between the ground-state levels m_g and m'_g also results in four-wave mixing gain on a transition $|F_g, m_g\rangle \rightarrow |F_e, m_e\rangle \rightarrow |F_g, m'_g\rangle \rightarrow |F_e, m'_e\rangle \rightarrow |F_g, m_g\rangle$ (figure 6(b)).

In such situations we observe a very pronounced threshold for collective emission into the resonator, occurring at free-space scattering rates per atom typically a factor of 10 larger than for large detuning (section 3.1). Furthermore, compared to the results for two-level atoms, the cavity-to-free-space emission ratio is limited to values near $\eta \approx 1$. This can be explained by the fact that stimulated Raman transitions saturate the inversion between the magnetic sublevels that is the origin of both the Raman and the four-wave mixing gain. This inversion has to be built up by scattering into free space, so that the ratio of stimulated Raman emission into the resonator to spontaneous Raman emission into free space cannot exceed unity. The four-wave mixing signal does not deplete the inversion, and allows for a cavity emission that exceeds the total free-space emission. To demonstrate that, as distinct from collective Rayleigh scattering, this collective Raman process involves multiple magnetic sublevels of the atoms, we apply a uniform magnetic field along the direction of the pump light's polarization and analyse the polarization and change in frequency of the emitted light (figure 6(c)). As expected, the emitted light consists of equal components of opposite circular polarization, whose frequencies vary linearly with the applied Zeeman shift.

A striking difference to the large-detuning limit, where only the centre-of-mass motion is strongly cooled, is that for the sample of multilevel atoms very efficient cooling of all degrees of freedom down to temperatures of a few microkelvin can be observed [19]. The forces on the atoms depend critically on the alignment of the counterpropagating pump beams, beyond the sensitivity expected to arise from the necessity to balance the radiation pressure. This strongly indicates that phase-matching and four-wave gain play a central role in the observed cooling forces.

The exact mechanism for the efficient multilevel-atom cooling is not well understood. Numerical simulations performed by Ritsch and co-workers [43] reproduce the observed large cooling forces, but do not provide direct insight into the cooling mechanism. Hafezi and Lukin have developed a model to calculate the forces in the simultaneous presence of Raman and four-wave mixing gain [44]. In this model, the cooling force arises from a delay in the atomic polarization of the moving atom, rather than a delay in the evolution of the cavity field [25]. The mechanism resembles an emission Doppler cooling mechanism, where the sideband asymmetry arises from an asymmetric gain for the red and blue Doppler sidebands (figure 2(b)). The validity of the approximations made in the model, and the conclusions of this model with respect to cooling rate, parameter dependence, and final temperature, will need to be experimentally verified.

5. Conclusion

The behaviour of atomic samples cooperatively interacting with light is a field of active experimental and theoretical study. This problem is of interest not only with respect to the laser cooling of arbitrary particles, but also in the context of quantum information processing and entanglement. Superradiant emission of light, and the associated self-organization of the atomic sample, automatically create large entangled states, since the emission process does not allow one, even in principle, to decide which atom emitted the photon. The resulting Dicke states are also at the heart of current experimental efforts [45–47] to create a conditional single-photon source from a many-atom sample [48].

References

- [1] Einstein A 1924 *Sitzungsber. Kgl. Preuss. Akad. Wiss.* 261
- [2] Bose S N 1924 *Z. Phys.* **26** 178
- [3] Anderson M H, Ensher J R, Matthews M R, Wieman C E and Cornell E A 1995 *Science* **269** 198
- [4] Bradley C C, Sackett C A, Tollett J J and Hulet R G 1995 *Phys. Rev. Lett.* **75** 1687
- [5] Davis K B, Mewes M O, Andrews M R, van Druten N J, Durfee D S, Kurn D M and Ketterle W 1995 *Phys. Rev. Lett.* **75** 3969
- [6] Cornell E A, Ketterle W and Wieman C E 2002 *Rev. Mod. Phys.* **74** 875 and references therein
- [7] Leggett A J 2001 *Rev. Mod. Phys.* **73** 307
- [8] Einstein A 1917 *Z. Phys.* **18** 121
- [9] Hänsch T W and Schawlow A L 1975 *Opt. Commun.* **13** 68
- [10] Wineland D J and Itano W M 1979 *Phys. Rev. A* **20** 1521
- [11] Chu S, Cohen-Tannoudji C and Phillips W D 1998 *Rev. Mod. Phys.* **70** 685
- [12] Einstein A 1905 *Ann. Phys.* **17** 549
- [13] Chu S, Bjorkholm J E, Ashkin A and Cable A 1986 *Phys. Rev. Lett.* **57** 314
- [14] Mossberg T W, Lewenstein M and Gauthier D J 1991 *Phys. Rev. Lett.* **67** 1723
- [15] Horak P, Hechenblaikner G, Gheri K M, Stecher H and Ritsch H 1997 *Phys. Rev. Lett.* **79** 4974
- [16] Hechenblaikner G, Gangl M, Horak P and Ritsch H 1998 *Phys. Rev. A* **58** 3030
- [17] Domokos P and Ritsch H 2002 *Phys. Rev. Lett.* **89** 253003
- [18] Domokos P and Ritsch H 2003 *J. Opt. Soc. Am. B* **20** 1098 and references therein
- [19] Chan H W, Black A T and Vuletić V 2003 *Phys. Rev. Lett.* **90** 063003
- [20] Nagorny B, Elsässer Th and Hemmerich A 2003 *Phys. Rev. Lett.* **91** 153003
- [21] Kruse D, von Cube C, Zimmermann C and Courteille Ph W 2003 *Phys. Rev. Lett.* **91** 183601
- [22] Black A T, Chan H W and Vuletić V 2003 *Phys. Rev. Lett.* **91** 203001
- [23] von Cube C, Slama S, Kruse D, Zimmermann C, Courteille Ph W, Robb G R M, Piovella N and Bonifacio R 2004 *Phys. Rev. Lett.* **93** 083601
- [24] Maunz P, Puppe T, Schuster I, Syassen N, Pinkse P W H and Rempe G 2004 *Nature* **428** 6978
- [25] Vuletić V and Chu S 2000 *Phys. Rev. Lett.* **84** 3787
- [26] Vuletić V, Chan H W and Black A T 2001 *Phys. Rev. A* **64** 033405
- [27] Purcell E M 1946 *Phys. Rev.* **69** 681
- [28] Ye J, Vernooy D W and Kimble J H 1999 *Phys. Rev. Lett.* **83** 4987
- [29] Münstermann P, Fischer T, Maunz P, Pinkse P W H and Rempe G 1999 *Phys. Rev. Lett.* **82** 3791
- [30] Dicke R H 1954 *Phys. Rev.* **93** 99
- [31] Raimond J M, Goy P, Gross M, Fabre C and Haroche S 1982 *Phys. Rev. Lett.* **49** 1924
- [32] Schneble D, Torii Y, Boyd M, Streed E W, Pritchard D E and Ketterle W 2003 *Science* **300** 475
- [33] Schneble D, Campbell G K, Streed E W, Boyd M, Pritchard D E and Ketterle W 2004 *Phys. Rev. A* **69** 041601(R)
- [34] Kaluzny Y, Goy P, Gross M, Raimond J M and Haroche S 1983 *Phys. Rev. Lett.* **51** 1175
- [35] Black A T, Chan H W and Vuletić V 2003 *18th Proc. Int. Conf. Atomic Physics (Cambridge)* (Singapore: World Scientific) p 91
- [36] Black A T, Chan H W and Vuletić V 2004 *16th Proc. Int. Conf. Laser Spectroscopy (Palm Cove)* (Singapore: World Scientific) p 345
- [37] Zippilli S, Morigi G and Ritsch H 2004 *Preprint quant-ph 0402152*
- [38] Robb G R M, Piovella N, Ferraro A, Bonifacio R, Courteille Ph W and Zimmermann C 2004 *Phys. Rev. A* **69** 041403(R)
- [39] Bonifacio R and De Salvo L 1994 *Nucl. Instrum. Methods Res. Sec. A* **341** 360
- [40] Bonifacio R, De Salvo L, Narducci M and D'Angelo E J 1994 *Phys. Rev. A* **50** 1716
- [41] Elsässer Th, Nagorny B and Hemmerich A 2004 *Phys. Rev. A* **69** 033403
- [42] Courtois J Y, Grynberg G, Lounis B and Verkerk P 1994 *Phys. Rev. Lett.* **72** 3017
- [43] Ritsch H 2004 Private communication
- [44] Hafezi M and Lukin M in preparation
- [45] Kuzmich A, Bowen W P, Boozer A D, Boca A, Chou C W, Duan L M and Kimble H J 2003 *Nature* **423** 731
- [46] Eisaman M D, Childress L, Andre A, Massou F, Zibrov A S and Lukin M D 2004 *Preprint quant-ph 0406093*
- [47] Chou C W, Polyakov S V, Kuzmich A and Kimble H J 2004 *Phys. Rev. Lett.* **92** 213601
- [48] Duan L M, Lukin M D, Cirac J I and Zoller P 2001 *Nature* **414** 413